Int. J. Solids Structures Vol. 30, No. 3, pp. 385–398, 1993
Printed in Great Britain.

0020–7683/93 $5.00+ .00

A SELF-CONSISTENT MODEL FOR MULTI-FIBER CRACK BRIDGING

WILLIAM S. SLAUGHTER†
Division of Applied Sciences, Harvard University, Cambridge, MA 02138, U.S.A.

(*Received* 19 *September* 1991; *in revised form* 1 *April* 1992)

Abstract—A self-consistent model for determining the equivalent spring stiffness in fiber crack-bridging problems is proposed. The model is compared with the shear-lag model for ideal bonding of the fiber–matrix interface, in which case the springs have a linear spring constant. A comparison is also made, in the homogeneous limit when fiber and matrix elastic properties are identical, with results from particle and ligament crack-bridging analyses. The self-consistent model is seen to agree with these other models. A simplified parametric equation is given which approximates the results over the considered range of material properties.

INTRODUCTION

A great deal of interest in recent years has centered around the subject of fiber-reinforced materials. This is due, largely, to experimental studies that have demonstrated that fiber-reinforcing can substantially increase the fracture toughness of ceramics, which are normally very brittle (Prewo and Brennan, 1980). It is anticipated that if ceramic materials can be adequately toughened, either through fiber-reinforcing or some other mechanism, the excellent thermal properties (and perhaps electrical properties) which they exhibit will provide a significant technological advance.

It has been demonstrated how a steady-state crack, growing normal to an aligned array of reinforcing fibers, can be modeled by analysing a configuration in which there are no fibers but a continuous distribution of springs restraining the two crack faces (Budiansky and Amazigo, 1989). The spring stress is a function of the crack opening displacement and is zero when the displacement is zero. The model material on which the springs act is assumed to be homogeneous and transversely isotropic with elastic constants equal to those of the composite. The critical energy release rate is modified to account for the increase in crack area due to the absence of fibers. Budiansky and Amazigo used this model to examine a semi-infinite crack growing through an infinite, reinforced material where the fibers break at some critical fiber stress. This condition results in a zone, starting at the crack-tip, in which fiber bridging is contained. This zone extends back to infinity as the critical fiber stress becomes large. The manner in which an "equivalent" spring strength is determined, so that the fracture toughness is the same for the model as it would be for the fiber-reinforced material, is the subject of this paper. Budiansky and Amazigo assumed fiber–matrix interface conditions in which sliding occurs when the interfacial shear stress reaches a maximum value, resulting in a nonlinear spring stiffness. Only the limiting condition of ideal bonding, in which the spring stiffness can be expressed as a linear spring constant, is considered here.

Budiansky and Amazigo used a shear-lag model, developed by Budiansky *et al.* (1986), to determine an equivalent spring stiffness for their model. A similar method was devised by Aveston and Kelly (1973). In the shear-lag model, a representative problem is examined in which a fiber is concentrically embedded in a cylindrical matrix. The ratio of fiber and matrix radii is chosen so that the fiber volume concentration of the composite is preserved. It is further supposed that all axial stresses in the matrix are concentrated at an intermediate, "effective" radius and that the volume of matrix between this effective radius and the fiber supports only shear stresses. The effective radius is chosen through complementary energy considerations. Alternatively, Aveston and Kelly defined the effective radius as that at which the axial displacement equals the average for the matrix, though they did not

† Current address: Department of Engineering, Trumpington Street, Cambridge CB2 1PZ, U.K.

explicitly solve for it. The result is an approximate solution for fiber and matrix stresses far downstream of the crack-tip from which an equivalent spring stiffness can be determined.

The assumptions of the shear-lag model result in a method that is adaptable to a wide range of fiber–matrix interface conditions. These include ideal bonding, sliding with constant frictional stress, Coulomb frictional sliding (Hutchinson and Jensen, 1990), and non-frictional debonding with a critical debonding energy release rate (Budiansky *et al.*, 1986). At the same time, however, it has not been shown to what extent these assumptions affect the accuracy of the results. For example, in the limit as fiber volume concentration tends to zero, no axial load is transferred between the fiber and matrix. This indicates that there *might* be some range of small fiber volume concentrations over which the shear-lag model is unsuitable.

Proposed here is a self-consistent model for determining the equivalent spring constant in fiber crack-bridging problems. Incorporated into this model is the method for analysing fiber load-diffusion problems that was developed by Slaughter and Sanders (1991). Also utilized is the assumption, made by Budiansky and Amazigo (1989), that the elastic field in the composite can be approximated by a homogeneous system. In contrast to the shear-lag model (which may be unreliable for small concentrations), the assumptions of this model tend to break down for high fiber volume concentrations. The two models should, therefore, provide a good check on each other.

SELF-CONSISTENT APPROXIMATION

Consider a semi-infinite, plane crack driven by an average far-field stress, $\bar{\sigma}$. The crack grows through an infinite matrix that is reinforced by an aligned array of fibers. The fibers are normal to the crack plane and the crack is presumed to grow around the fibers, leaving them intact in its wake. Downstream of the crack tip the elastic field approaches that represented in Fig. 1. In this three-dimensional field, the fibers are of radius a and the fiber volume concentration is c. Both the fibers and matrix are homogeneous and isotropic, linear elastic solids with Young's modulus and Poisson's ratio taken, respectively, to be E_f and ν_f for the fibers and E_m and ν_m for the matrix. The z-direction is defined as that in which the applied stress, $\bar{\sigma}$, acts and in which the fibers are aligned, i.e. normal to the crack, with $z = 0$ at the crack plane.

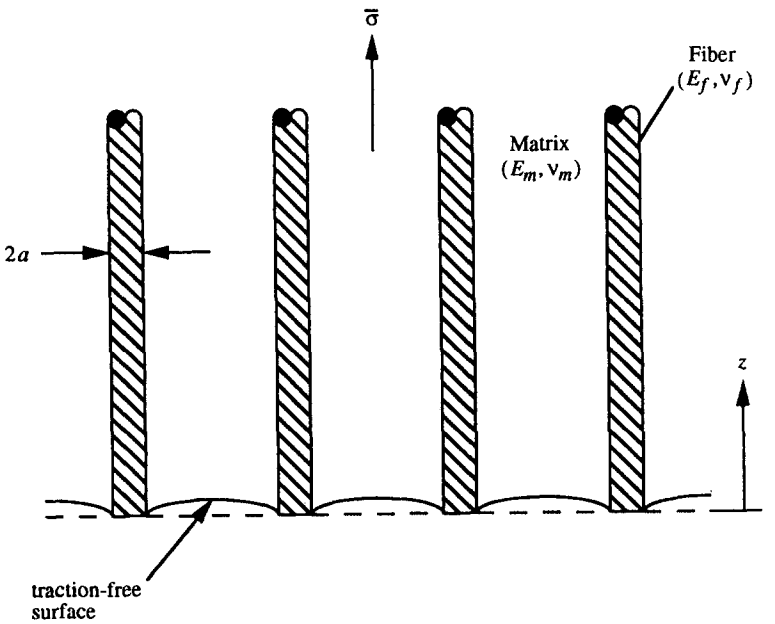

Fig. 1. Elastic field far behind the crack-tip in a fiber crack-bridging problem in which the fibers are aligned and remain unbroken. The fiber–matrix interface is ideally bonded.

The overall elastic response of an aligned fiber composite can be expressed in terms of transversely isotropic elastic moduli. A theory for approximating these moduli, for an arbitrary aligned fiber composite, has been developed using self-consistent arguments (Hill, 1965). The five moduli are, in this instance, most conveniently given as the stiffnesses C_{11}, C_{33}, C_{12}, C_{13} and C_{44}. The composite Young's modulus for axial extension,

$$E_z = C_{33} - 2C_{13}^2/(C_{11}+C_{12}) \approx cE_f + (1-c)E_m,$$

will also prove useful. For a more detailed discussion of the overall elastic moduli see Appendix A. Referring to Fig. 1, the following conditions on axial displacement, w, and radial and axial stress, σ_r and σ_z, respectively, are noted:

$$\begin{aligned} &\text{at } z = 0: \quad w = 0, \quad \sigma_z^m = 0, \quad \sigma_z = \frac{1}{c}\bar{\sigma}, \\ &\text{at } z \to \infty: \quad \sigma_r \approx \sigma_r^m \approx 0, \quad \sigma_z^m \approx E_m\bar{\varepsilon}, \quad \sigma_z = E_f\bar{\varepsilon}, \end{aligned} \tag{1}$$

where $\bar{\varepsilon} \equiv \bar{\sigma}/E_z$ is the uniform, far-field axial strain. Matrix quantities are denoted by superscript m while fiber quantities are without denotation and represent the average over a fiber cross-section. It is assumed that the elastic response of a fiber, in an aligned fiber composite, can be approximated by the response of a single fiber embedded in a homogeneous, transversely isotropic material with elastic moduli equal to those of the composite.

The contribution to the far-field axial displacement, due to the passage of the crack in the composite, is given by

$$\Delta = \lim_{L\to\infty} \int_0^L (\varepsilon_z - \bar{\varepsilon})\, dz. \tag{2}$$

The equivalent spring constant, k, that is needed to analyse the fracture toughening effect of the fiber reinforcement, using Budiansky and Amazigo's method, relates this displacement to the far-field stress,

$$\bar{\sigma} = k\Delta. \tag{3}$$

For ideal bonding of the fiber–matrix interface, k depends only on material properties and the fiber volume concentration, c. This spring constant can be used to model the effects of fiber crack bridging. More specifically, in this case, it is assumed that the effect on the elastic response of a fiber in the composite, due to crack bridging by all other fibers, can be approximated by that due to a continuous distribution of springs, relating normal tractions to surface displacements via the linear spring stiffness, k.

The self-consistent method for determining k makes use of both the aforementioned methods for approximating the effects of discrete fibers. This results in the assumption that the reaction in one of the fibers shown in Fig. 1 can be modeled by the single fiber problem shown in Fig. 2. In this problem the matrix has the elastic properties of the fiber composite. The fiber properties remain unchanged. The surface at $z = 0$ is restrained by the linear springs with equivalent spring constant k, as defined above. A polar coordinate system is defined with r measured from the fiber center. This leads to the following modifications of the conditions given in eqns (1):

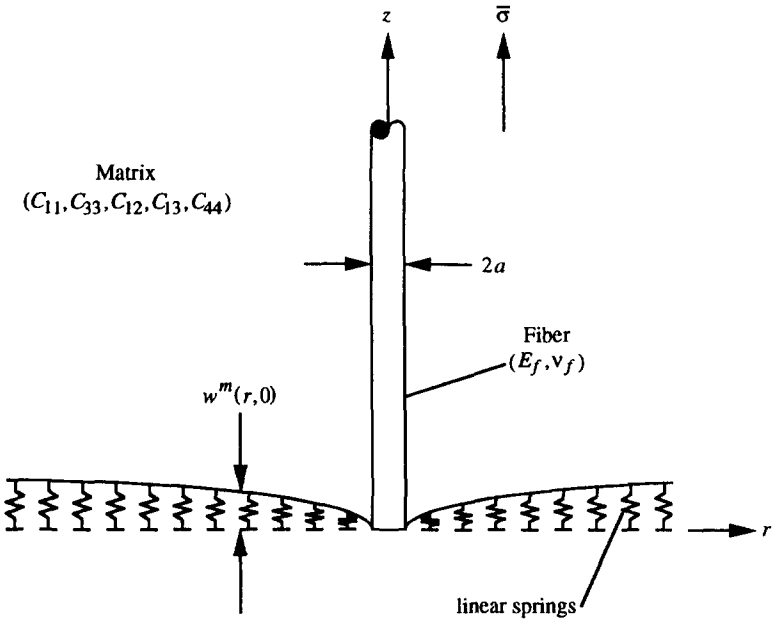

Fig. 2. Self-consistent approximation to the fiber crack-bridging problem. The matrix has the transversely isotropic elastic properties of the fiber–matrix composite.

$$\text{at } z = 0: \quad w = 0, \quad \sigma_z^{\mathrm{m}} = kw^{\mathrm{m}}, \quad \sigma_z = \frac{1}{c}\bar{\sigma},$$

$$\text{at } z \to \infty: \quad \sigma_r \approx \sigma_r^{\mathrm{m}} \approx 0, \quad \sigma_z^{\mathrm{m}} = \bar{\sigma}, \quad \sigma_z = E_{\mathrm{f}}\bar{\varepsilon} = \frac{E_{\mathrm{f}}}{E_z}\bar{\sigma}, \tag{4}$$

along with the observation that at $z = 0$

$$\lim_{r \to \infty} w^{\mathrm{m}} = \Delta. \tag{5}$$

For a given fiber volume concentration, c, which spring constant, k, will cause the zero fiber displacement constraint at $z = 0$, given in eqns (4), to be satisfied? A similar self-consistent model, for unbroken ligaments between crack faces in a homogeneous, isotropic material, was considered by Rose (1987). For numerical reasons to come later it will prove advantageous to consider the inverse form of this; for a given spring constant k (and given material properties), what fiber volume concentration c will cause the zero fiber displacement constraint at $z = 0$ to be satisfied?

The elastic field shown in Fig. 2 has nonzero components at $(r, z) \to \infty$. This is eliminated by superposing a uniform compressive strain $\varepsilon_z = \varepsilon_z^{\mathrm{m}} = -\bar{\varepsilon}$, $\sigma_z^{\mathrm{m}} = -\bar{\sigma}$, $\sigma_z = -E_{\mathrm{f}}\bar{\sigma}/E_z$. The problem becomes that shown in Fig. 3. Displacements and stresses now vanish at infinity, while at $z = 0$

$$\begin{aligned} w &= -\Delta, \\ \sigma_z^{\mathrm{m}} &= kw^{\mathrm{m}}, \\ \sigma_z &\equiv \frac{F}{\pi a^2} = \left(\frac{1}{c} - \frac{E_{\mathrm{f}}}{E_z}\right)\bar{\sigma}. \end{aligned} \tag{6}$$

This superposition facilitates the application of the fiber load-diffusion analysis method introduced in Slaughter and Sanders (1991). F is defined as the load on the end of the fiber. For a given k, what fiber volume concentration c will result in the satisfaction of eqns (6)?

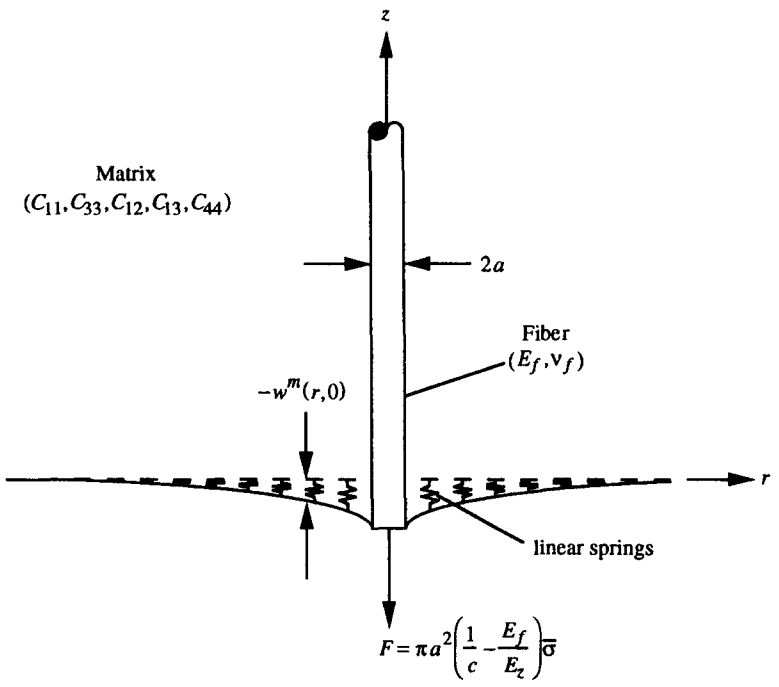

Fig. 3. Self-consistent approximation to the fiber crack-bridging problem plus the superposition of a uniform axial strain to nullify far-field stresses.

THE EQUIVALENT SPRING CONSTANT

In solving for the equivalent spring constant, k, in Fig. 3, the model for load-transfer from an embedded fiber to an elastic matrix, introduced in Slaughter and Sanders (1991), is adopted. The fiber is approximated as an axisymmetric, elastic rod with axial stress σ_z. Shear strains in the fiber are ignored and $\varepsilon_\theta = \varepsilon_r$, ε_z, $\sigma_\theta = \sigma_r$ and σ_z are functions of z only. Constitutive equations for the fiber reduce to the following,

$$\sigma_z = E_f\varepsilon_z + 2\nu_f\sigma_r, \tag{7}$$

$$E_f\varepsilon_\theta + \nu_f E_f\varepsilon_z - (1-2\nu_f)(1+\nu_f)\sigma_r = 0. \tag{8}$$

Forces acting on the fiber are an applied load F, at the fiber end, and bonding tractions with the matrix, $\tau = \tau_{rz}^m(a,z)$ and $\sigma_r = \sigma_r^m(a,z)$, along the fiber–matrix interface at $r = a$. The fiber is in equilibrium if, for all $z \geqslant 0$,

$$\pi a^2\sigma_z + 2\pi a\int_0^z \tau\,dz' = F. \tag{9}$$

The fiber quantities ε_θ, σ_r and ε_z remain to be related to quantities in the matrix.

In contrast to the problem of load-transfer from a single fiber to a semi-infinite matrix analysed in Slaughter and Sanders (1991), compressive normal tractions, $t(r) \equiv -\sigma_z^m(r,0)$, act along the surface of the mattrix at $z = 0$ where

$$t(r) = -kw^m(r,0). \tag{10}$$

Over-all equilibrium for the fiber–matrix system requires that

$$2\pi \int_a^\infty t(r) r \, dr = F. \tag{11}$$

In addition, the matrix is transversely isotropic with elastic moduli C_{11}, C_{33}, C_{12}, C_{13} and C_{44}. Elliott (1948, 1949) showed how the elastic field in such a material can be expressed in terms of two "harmonic" functions, ϕ_1 and ϕ_2, where

$$\left(\nabla_1^2 + \mu_i \frac{\partial^2}{\partial z^2}\right)\phi_i = 0, \quad (i = 1, 2), \tag{12}$$

and μ_1 and μ_2 are the roots of

$$C_{11}C_{44}\mu^2 + [C_{13}(2C_{44} + C_{13}) - C_{11}C_{33}]\mu + C_{33}C_{44} = 0. \tag{13}$$

For axially symmetric fields

$$\nabla_1^2 \equiv \frac{\partial^2}{\partial r^2} + \frac{1}{r}\frac{\partial}{\partial r} \tag{14}$$

and the radial and axial displacements, u and w, respectively, are given by

$$u = \frac{\partial \phi_1}{\partial r} + \frac{\partial \phi_2}{\partial r}, \quad w = \kappa_1 \frac{\partial \phi_1}{\partial z} + \kappa_2 \frac{\partial \phi_2}{\partial z}, \tag{15}$$

where

$$\kappa_i \equiv \frac{C_{11}\mu_i - C_{44}}{C_{13} + C_{44}}, \quad (i = 1, 2). \tag{16}$$

The roots of eqn (13) are either real and positive, in which case ϕ_1 and ϕ_2 are real, or they are complex conjugates, in which case ϕ_1 and ϕ_2 are complex conjugates as well.

The elastic field in this problem is approximated by that due to a point force of magnitude F, acting at the origin in the negative z-direction, along with distributions along the z-axis of point forces and point dilatations, $p(z)$ and $q(z)$, and the traction distribution, $t(r)$. The point forces are in the negative z-direction and the point force distribution must be self-equilibrating;

$$\int_0^\infty p(\zeta) \, d\zeta = 0. \tag{17}$$

In terms of the Elliott harmonic functions, this approximate field is expressed as

$$\phi_i = \int_0^\infty \{\phi_i^A(r, z, \zeta)[F\delta(\zeta) + p(\zeta)] + \phi_i^B(r, z, \zeta) q(\zeta)\} \, d\zeta + \int_a^\infty \phi_i^C(r, z, \rho) t(\rho) \, d\rho, \quad (i = 1, 2), \tag{18}$$

where $\phi_i^A(r, z, \zeta)$ and $\phi_i^B(r, z, \zeta)$ are the elastic solutions at (r, z) for a point force and a point dilatation, respectively, acting at $(0, \zeta)$ and $\phi_i^C(r, z, \rho)$ is the elastic solution at (r, z) for a ring of point forces at $(\rho, 0)$. $\delta(z)$ is the Dirac function. See Appendix B for a more detailed discussion and explicit expressions for these and following kernel functions. ϕ_i^A and ϕ_i^B are well behaved analytic functions for $r \neq 0$. ϕ_i^C has an integrable singularity, when $z = 0$, at $r = \rho$. As a result, the elastic field given by eqn (18) has real, analytic displacements, strains, and stresses when $r \neq 0$. Each of these quantities is expressible, through eqns (15) and (18), as integrals of known kernel functions times the unknown distributions.

The governing equations for this problem are (8), (9) and (10). Over-all equilibrium of the problem, eqn (11), and the self-equilibrating condition on the point force distribution, eqn (17), offer additional constraint on the solution. Equation (7) is used to eliminate σ_z from (9). In order to express the governing equations in terms of the unknown distributions, the fiber quantities ε_θ, σ_r and ε_z need to be related to quantities in the matrix. Following the method in the solution of the single fiber problem (Slaughter and Sanders, 1991),

$$\varepsilon_\theta = \frac{1}{a} u^m(a, z), \tag{19}$$

$$\sigma_r = \sigma_r^m(a, z). \tag{20}$$

For the axial fiber strain,

$$\varepsilon_z = \varepsilon_z^m(a, z), \tag{21}$$

when used in eqn (8), while

$$\varepsilon_z = \frac{1}{\pi a^2 E_f} \int_0^\infty H(z-\zeta)\left[1 - \operatorname{erf}\left(\frac{z-\zeta}{a}\right)\right][F\delta(\zeta) + p(\zeta)]\,d\zeta + \varepsilon_z^m(a, z), \tag{22}$$

when used in eqn (9), where $H(z)$ is the Heaviside step function. The relation (22) compensates for the discontinuity in axial strain in the fiber across an applied step loading. The discontinuity is necessary under the elastic rod approximation if σ_r is assumed to be continuous.

Using the relationship between fiber and matrix quantities, established in eqns (19) through (22), and the expression for the elastic field in the matrix, eqn (18), the governing equations can be rewritten as coupled integral equations for the unknown distributions $p(z)$, $q(z)$ and $t(r)$. Non-dimensionalizing in a and F such that $k \Rightarrow E_f k/a$,

$$\int_0^z p(\zeta)\,d\zeta + \int_0^\infty [\Gamma_{11}(z, \zeta)p(\zeta) + \Gamma_{12}(z, \zeta)q(\zeta)]\,d\zeta + \int_1^\infty \Gamma_{13}(z, \rho)t(\rho)\,d\rho = -\Gamma_{11}(z, 0), \tag{23}$$

$$\int_0^\infty [\Gamma_{21}(z, \zeta)p(\zeta) + \Gamma_{22}(z, \zeta)q(\zeta)]\,d\zeta + \int_1^\infty \Gamma_{23}(z, \rho)t(\rho)\,d\rho = -\Gamma_{21}(z, 0), \tag{24}$$

$$\int_0^\infty [\Gamma_{31}(r, \zeta)p(\zeta) + \Gamma_{32}(r, \zeta)q(\zeta)]\,d\zeta + \frac{\pi}{k} t(r) + \int_1^\infty \Gamma_{33}(r, \rho)t(\rho)\,d\rho = -\Gamma_{31}(r, 0), \tag{25}$$

where the kernels $\Gamma_{\alpha\beta}$ $(\alpha, \beta = 1, 2, 3)$ are real functions. See Appendix B for explicit expressions for the kernels and non-dimensionalizations. All subsequent expressions are in non-dimensional form. To solve for the distributions, the system of coupled integral equations (23), (24) and (25) is reduced to a set of discrete linear equations. The integrals are approximated using the mapped Gauss–Legendre rule and each equation is enforced at the quadrature points, in accordance with the Nystrom method (Delves and Mohamed, 1985). The constraints (11) and (17), which in non-dimensional form are

$$\int_1^\infty t(\rho)\rho \, d\rho = \frac{1}{2\pi}, \tag{26}$$

$$\int_0^\infty p(\zeta) \, d\zeta = 0, \tag{27}$$

are added to this set of linear equations. The resulting system exhibits some ill-posed tendencies due to the nature of the integral equations. These problems are dealt with by using singular value decomposition (SVD) to solve the set of linear equations.

To solve for the fiber volume concentration, c, that corresponds to a given spring constant, k, requires an iterative approach. The transversely isotropic material stiffnesses of the matrix depend on c and, therefore, so do the kernel functions, $\Gamma_{\alpha\beta}$ ($\alpha, \beta = 1, 2, 3$). If an estimate of c is used and the distributions solved for, then a new estimate for c can be calculated from the definition of the load applied to the end of the fiber [eqn (6)]

$$c = k\Delta\left[1 + \left(\frac{E_f}{E_z}\right)k\Delta\right]^{-1}, \tag{28}$$

where $\Delta = w^m(1,0)$ and

$$w^m(1,0) = \Gamma_{31}(r,0) + \int_0^\infty [\Gamma_{31}(r,\zeta)p(\zeta) + \Gamma_{32}(r,\zeta)q(\zeta)] \, d\zeta + \int_1^\infty \Gamma_{33}(r,\rho)t(\rho) \, d\rho. \tag{29}$$

Equation (29) is theoretically equivalent to $w^m(r,0) = -\pi t(r)/k$ but converges more steadily during numerical analysis. In this way, the estimate for c is refined until there is convergence.

The results from this analysis are compared with those from the shear-lag model (Budiansky and Amazigo, 1989) in the instance that the fiber and matrix remain ideally bonded. In addition, in the limit that fiber and matrix elastic properties are the same, comparison can be made with Rose's analysis for unbroken ligaments bridging the crack faces (Rose, 1987) as well as with an analysis of crack bridging by particulate reinforcements (Budiansky *et al.*, 1988). Comparisons for the case when fiber and matrix elastic properties are the same are shown in Fig. 4 and those for dissimilar fiber and matrix elastic properties

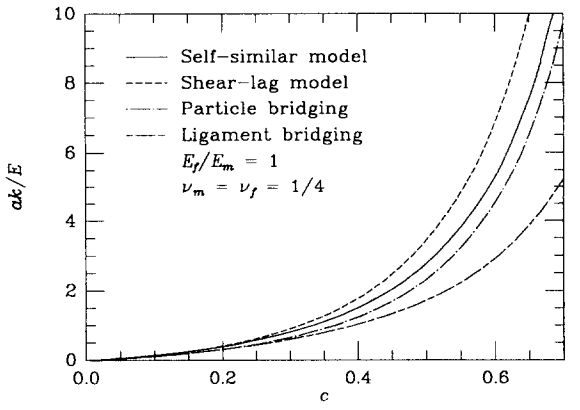

Fig. 4. The equivalent spring constant versus fiber volume concentration in the homogeneous limit when the fiber and matrix elastic properties coincide. In addition to the self-consistent model, results from the shear-lag model (Budiansky and Amazigo, 1989), a particle crack-bridging analysis (Budiansky *et al.*, 1988), and a ligament crack-bridging analysis (Rose, 1987) are plotted.

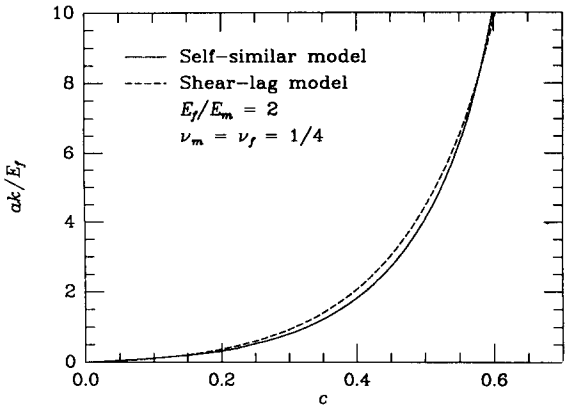

Fig. 5. The equivalent spring constant versus fiber volume concentration for the self-consistent model and the shear-lag model (Budiansky and Amazigo, 1989) when the ratio of the fiber to matrix Young's moduli is 2 and both Poisson's ratios are 1/4.

are shown in Figs 5–7. It is noted that variations in the Poisson's ratio of either the fiber or matrix have little effect on any of these models. The following parametric curve-fitting equation approximates the results from the self-consistent model for the equivalent spring constant as a function of fiber volume concentration:

$$k = \alpha c(1-c)^{\gamma}, \tag{30}$$

where

$$\alpha = 2.8\left(\frac{E_f}{E_m}+1\right)^{-1}, \tag{31}$$

$$\gamma = 0.73-2.73\sqrt{\frac{E_f}{E_m}}. \tag{32}$$

Plots of this approximate formula are given, along with results from the self-consistent analysis, in Fig. 8.

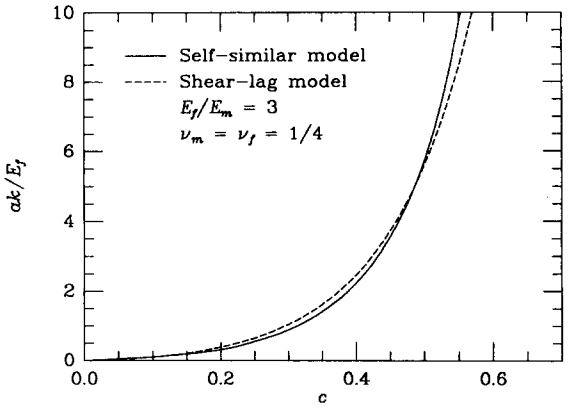

Fig. 6. The equivalent spring constant versus fiber volume concentration for the self-consistent model and the shear-lag model (Budiansky and Amazigo, 1989) when the ratio of the fiber to matrix Young's moduli is 3 and both Poisson's ratios are 1/4.

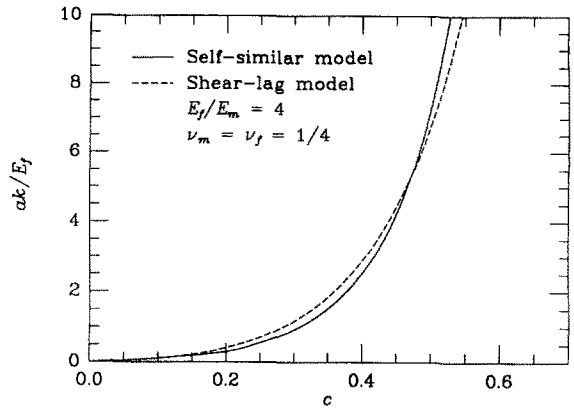

Fig. 7. The equivalent spring constant versus fiber volume concentration for the self-consistent model and the shear-lag model (Budiansky and Amazigo, 1989) when the ratio of the fiber to matrix Young's moduli is 4 and both Poisson's ratios are 1/4.

CONCLUDING REMARKS

It can be seen in Fig. 4 that, in the homogeneous limit of equivalent fiber and matrix material properties, the self-consistent model is in agreement with other available models. Surprisingly, the model developed by Rose (1987) for crack bridging by equiaxed ligaments, which is conceptually most like the self-consistent model, exhibits the greatest divergence in results. This is due to different assumptions on how discrete crack-bridging ligaments can be modeled by continuous spring distributions and how the resulting single ligament problem (or single fiber problem in this paper) is approximately solved. Both the shear-lag model and the particulate reinforcement model agree fairly well with the self-consistent model.

An examination of Figs 5–7 shows that the self-consistent and shear-lag models continue to give closely matched results throughout the range of material properties considered. The proposition that the two might be best applied to different ranges of fiber volume concentrations is not borne out. The results shown here indicate that either model would be suitable for the full range of concentrations. Ease of use suggests that, as long as only ideal bonding of the fiber–matrix interface is considered, the parametric equation (30), derived from the self-consistent model, may prove more convenient. It should be noted, however, that effective toughening in fiber-reinforced ceramics is seen to be associated with debonding of the fiber–matrix interface and fiber pull-out. The shear-lag model continues to enjoy a considerable advantage in calculating the nonlinear spring stiffnesses that follow from these conditions. These results serve to confirm the reliability of the shear-lag model when extended into problems of complicated fiber–matrix interface conditions.

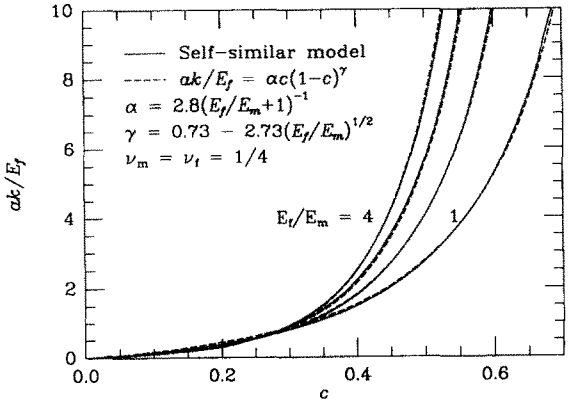

Fig. 8. The equivalent spring constant versus fiber volume concentration for the self-consistent model and the parametric curve-fitting equation.

Acknowledgements—This work was supported in part by the DARPA University Research Initiative (Subagreement P.O. VB38639-0 with the University of California, Santa Barbara, ONR Prime Contract N00014-86-K-0753), the Office of Naval Research (Contract N00014-90-J-1377), and the Division of Applied Sciences, Harvard University.

REFERENCES

Aveston, J. and Kelly, A. (1973). Theory of multiple fracture of fibrous composites. *J. Mater. Sci.* **8,** 352–362.

Budiansky, B. and Amazigo, J. C. (1989). Toughening by aligned, frictionally constrained fibers. *J. Mech. Phys. Solids* **37,** 93–109.

Budiansky, B., Amazigo, J. C. and Evans, A. G. (1988). Small-scale crack bridging and the fracture toughness of particulate-reinforced ceramics. *J. Mech. Phys. Solids* **36,** 167–187.

Budiansky, B., Hutchinson, J. W. and Evans, A. G. (1986). Matrix fracture in fiber-reinforced ceramics. *J. Mech. Phys. Solids* **34,** 167–189.

Delves, L. M. and Mohamed, J. L. (1985). *Computational Methods for Integral Equations.* Cambridge University Press, Cambridge.

Elliott, H. A. (1948). Three dimensional stress distributions in hexagonal aeolotropic crystals. *Proc. Cambridge Phil. Soc.* **44,** 522–533.

Elliott, H. A. (1949). Axial symmetric stress distributions in aeolotropic hexagonal crystals. The problem of the plane and related problems. *Proc. Cambridge Phil. Soc.* **45,** 621–630.

Hill, R. (1964). Theory of mechanical properties of fibre-strengthened materials: I. Elastic behaviour. *J. Mech. Phys. Solids* **12,** 199–212.

Hill, R. (1965). Theory of mechanical properties of fibre-strengthened materials: III. Self-consistent model. *J. Mech. Phys. Solids* **13,** 189–198.

Hutchinson, J. W. and Jensen, H. M. (1990). Models of fiber debonding and pullout in brittle composites with friction. *Mech. Mater.* **9,** 139–163.

Prewo, K. M. and Brennan, J. J. (1980). High-strength silicon carbide fiber-reinforced glass-matrix composites. *J. Mater. Sci.* **15,** 463–468.

Rose, L. R. F. (1987). Effective spring constant for unbroken ligaments between crack faces. *Int. J. Fract.* **33,** 145–152.

Shield, R. T. (1951). Notes on problems in hexagonal aeolotropic materials. *Proc. Cambridge Phil. Soc.* **47,** 401–409.

Slaughter, W. S. and Sanders, J. L. (1991). A model for load-diffusion from an embedded fiber to an elastic matrix. *Int. J. Solids Structures* **28,** 1041–1052.

APPENDIX A

Approximate composite elastic moduli

Hill (1965) used a self-consistent model to determine approximately the composite elastic moduli of fiber-reinforced materials. This approximation is independent of the spatial arrangement of the fibers. The only requirement is that the fibers be perfectly aligned and the composite exhibit statistical homogeneity. Hill showed further that the results from this model fall within bounds established as the best possible without considering detailed geometry (Hill, 1964). The composite is transversely isotropic with rigidity for transverse shearing over any axial plane, η; plane-strain bulk modulus for lateral dilation without fiber extension, γ; Young's modulus and Poisson's ratio under uniaxial loading, E_z and ν_{zr}; and rigidity for longitudinal shearing over any axial plane, G. The shearing rigidities are given by the positive roots of

$$\frac{c\gamma_f}{\gamma_f+\eta}+\frac{(1-c)\gamma_m}{\gamma_m+\eta}=2\left[\frac{c\eta_m}{\eta_m-\eta}+\frac{(1-c)\eta_f}{\eta_f-\eta}\right], \tag{A1}$$

$$\frac{c}{G-G_m}+\frac{1-c}{G-G_f}=\frac{1}{2G}, \tag{A2}$$

where subscript f and m signify fiber and matrix moduli, respectively, which for isotropic materials are given in terms of the isotropic Young's moduli, E, and Poisson's ratio, ν, by

$$\eta = G = \frac{E}{2(1+\nu)}, \tag{A3}$$

$$\gamma = \frac{E}{2(1+\nu)(1-2\nu)}. \tag{A4}$$

Using the result from (A1) then the remaining composite moduli are

$$E_z = cE_f+(1-c)E_m+4c(1-c)(\nu_f-\nu_m)^2\left(\frac{c}{\gamma_m}+\frac{1-c}{\gamma_f}+\frac{1}{\eta}\right)^{-1}, \tag{A5}$$

$$\nu_{zr} = c\nu_f+(1-c)\nu_m+c(1-c)(\nu_f-\nu_m)\left(\frac{1}{\gamma_m}-\frac{1}{\gamma_f}\right)\left(\frac{c}{\gamma_m}+\frac{1-c}{\gamma_f}+\frac{1}{\eta}\right)^{-1}, \tag{A6}$$

$$\gamma = \left(\frac{c}{\gamma_f+\eta}+\frac{1-c}{\gamma_m+\eta}\right)^{-1}-\eta. \tag{A7}$$

The composite stiffnesses are defined so that

$$\begin{bmatrix}\sigma_r\\ \sigma_\theta\\ \sigma_z\\ \tau_{\theta z}\\ \tau_{zr}\\ \tau_{r\theta}\end{bmatrix} = \begin{bmatrix}C_{11} & C_{12} & C_{13} & 0 & 0 & 0\\ C_{12} & C_{11} & C_{13} & 0 & 0 & 0\\ C_{13} & C_{13} & C_{33} & 0 & 0 & 0\\ 0 & 0 & 0 & 2C_{44} & 0 & 0\\ 0 & 0 & 0 & 0 & 2C_{44} & 0\\ 0 & 0 & 0 & 0 & 0 & C_{11}-C_{12}\end{bmatrix}\begin{bmatrix}\varepsilon_r\\ \varepsilon_\theta\\ \varepsilon_z\\ \varepsilon_{\theta z}\\ \varepsilon_{zr}\\ \varepsilon_{r\theta}\end{bmatrix}. \tag{A8}$$

In terms of the moduli used by Hill the stiffnesses are

$$C_{11} = \gamma+\eta, \tag{A9}$$

$$C_{12} = \gamma-\eta, \tag{A10}$$

$$C_{13} = 2\gamma\nu_{zr}, \tag{A11}$$

$$C_{33} = E_z+4\gamma\nu_{zr}^2, \tag{A12}$$

$$C_{44} = G. \tag{A13}$$

APPENDIX B

Singular solutions in a transversely isotropic elastic half-space

The solution for a point force acting in a transversely isotropic half-space has been previously studied (Shield, 1951). The solution for a unit force acting at $(r, z) = (0, \zeta)$ in the negative z-direction as required in eqn (18) is given by

$$\phi_1^{\wedge} = \frac{-P}{8\pi(\mu_1-\mu_2)}\left[\ln\left(\frac{R_1+z_1-\zeta_1}{R_1-z_1+\zeta_1}\right)-\ln\left(\frac{\bar{R}_1+z_1+\zeta_1}{\bar{R}_1-z_1-\zeta_1}\right)\right]-\frac{P}{2\pi\beta(\mu_1-\mu_2)}\left[\frac{\kappa_1C_{33}-\mu_1C_{13}}{(1+\kappa_1)\sqrt{\mu_1}}\ln(\bar{R}_1+z_1+\zeta_1)\right.$$
$$\left.-\frac{\kappa_2C_{33}-\mu_2C_{13}}{(1+\kappa_1)\mu_2}\sqrt{\mu_1}\ln(\delta_{12}+z_1+\zeta_2)\right], \tag{B1}$$

$$\phi_2^{\wedge} = \frac{P}{8\pi(\mu_1-\mu_2)}\left[\ln\left(\frac{R_2+z_2-\zeta_2}{R_2-z_2+\zeta_2}\right)-\ln\left(\frac{\bar{R}_2+z_2+\zeta_2}{\bar{R}_2-z_2-\zeta_2}\right)\right]+\frac{P}{2\pi\beta(\mu_1-\mu_2)}\left[\frac{\kappa_1C_{33}-\mu_1C_{13}}{(1+\kappa_2)\mu_1}\sqrt{\mu_2}\ln(\delta_{21}+z_2+\zeta_1)\right.$$
$$\left.-\frac{\kappa_2C_{33}-\mu_2C_{13}}{(1+\kappa_2)\sqrt{\mu_2}}\ln(\bar{R}_2+z_2+\zeta_2)\right], \tag{B2}$$

where

$$P = \frac{C_{13}+C_{44}}{C_{11}C_{44}}, \tag{B3}$$

$$\beta = \frac{\kappa_1C_{33}-\mu_1C_{13}}{(1+\kappa_1)\sqrt{\mu_1}}-\frac{\kappa_2C_{33}-\mu_2C_{13}}{(1+\kappa_2)\sqrt{\mu_2}}, \tag{B4}$$

$$z_i = \frac{z}{\sqrt{\mu_i}}, \quad \zeta_i = \frac{\zeta}{\sqrt{\mu_i}}, \tag{B5}$$

$$R_i = \sqrt{r^2+(z_i-\zeta_i)^2}, \quad \bar{R}_i = \sqrt{r^2+(z_i+\zeta_i)^2}, \tag{B6}$$

$$\delta_{ij} = \sqrt{r^2+(z_i+\zeta_j)^2}. \tag{B7}$$

Recall the definitions of μ_i and κ_i in eqns (13) and (16).

No solution for a point dilatation was found in the literature. Therefore, with the nature of the self-consistent model considered, a unit point "dilatation" at $(0, \zeta)$ is defined such that the net normal displacement through an infinitely long circular cylinder, with centroidal axis coincident with the z-axis, approaches unity as the radius approaches zero. The elastic field is axisymmetric. This condition is not sufficient to define a unique solution. The solution used in this application, chosen for convenience, is

$$\phi_1^B = \frac{-1}{4\pi(\sqrt{\mu_1}+\sqrt{\mu_2})}\left[\frac{1}{R_1}+\left(1+\frac{a_1 b_1}{\beta}\right)\frac{1}{\tilde{R}_1}+\left(\frac{a_1 b_2}{\beta}\right)\frac{1}{\delta_{12}}\right], \tag{B8}$$

$$\phi_2^B = \frac{-1}{4\pi(\sqrt{\mu_1}+\sqrt{\mu_2})}\left[\frac{1}{R_2}+\left(1-\frac{a_2 b_2}{\beta}\right)\frac{1}{\tilde{R}_2}-\left(\frac{a_2 b_1}{\beta}\right)\frac{1}{\delta_{21}}\right], \tag{B9}$$

where

$$a_i = \frac{2\sqrt{\mu_i}}{1+\kappa_i}, \quad b_i = C_{13}-C_{33}\frac{\kappa_i}{\mu_i}. \tag{B10}$$

The solution for a circular ring of compressive normal tractions of radius ρ on the surface $z = 0$ can be derived from the point force solution [eqns (B1) and (B2)]. The resulting elastic field is given by

$$\phi_1^C = \frac{1}{\pi\beta}\left(\frac{\sqrt{\mu_1}}{1+\kappa_1}\right)\int_0^\pi \ln(\tilde{R}_1+z_1)\rho\,\mathrm{d}\theta, \tag{B11}$$

$$\phi_2^C = \frac{-1}{\pi\beta}\left(\frac{\sqrt{\mu_2}}{1+\kappa_2}\right)\int_0^\pi \ln(\tilde{R}_2+z_2)\rho\,\mathrm{d}\theta, \tag{B12}$$

where

$$\tilde{R}_i = \sqrt{\tilde{r}^2+z_i^2}, \quad \tilde{r}^2 = r^2+\rho^2-2r\rho\cos\theta. \tag{B13}$$

This ring has a net force of $2\pi\rho$.

Expressions for required elastic quantities

Listed below are those elastic quantities that are needed for the implementation of the self-consistent model. They are given in terms of the Elliott "harmonic" functions ϕ_1 and ϕ_2 as defined in eqns (12)–(16):

$$u = \frac{\partial}{\partial r}(\phi_1+\phi_2), \tag{B14}$$

$$\varepsilon_z = \frac{\partial^2}{\partial z^2}(\kappa_1\phi_1+\kappa_2\phi_2), \tag{B15}$$

$$\tau_{rz} = C_{44}\left[(1+\kappa_1)\frac{\partial^2\phi_1}{\partial r\,\partial z}+(1+\kappa_2)\frac{\partial^2\phi_2}{\partial r\,\partial z}\right], \tag{B16}$$

$$\sigma_r = \left(C_{11}\frac{\partial^2}{\partial r^2}+C_{12}\frac{1}{r}\frac{\partial}{\partial r}\right)(\phi_1+\phi_2)+C_{13}\frac{\partial^2}{\partial z^2}(\kappa_1\phi_1+\kappa_2\phi_2). \tag{B17}$$

Non-dimensionalizations and kernels for the coupled integral equations

The kernel functions for the three integral equations (23)–(25) are arrived at by substituting (B14)–(B17) [with ϕ_1 and ϕ_2 given by (18)] into the governing equations (8)–(10) using the fiber–matrix relations (19)–(22). To non-dimensionalize with a and F the following substitutions are made:

$$z \to az, \quad \zeta \to a\zeta, \quad r \to ar, \quad \rho \to a\rho, \quad k \to \frac{E_f}{a}k, \quad p(\zeta) \to \frac{F}{a}p(\zeta),$$

$$q(\zeta) \to \frac{F}{E_f}q(\zeta), \quad t(\rho) \to \frac{F}{a^2}t(\rho), \quad \phi_i^A \to \frac{1}{\pi E_f}\phi_i^A, \quad \phi_i^B \to \frac{1}{\pi a}\phi_i^B, \quad \text{and} \quad \phi_i^C \to \frac{a}{\pi E_f}\phi_i^C.$$

The resulting expressions for the kernel functions are

$$\Gamma_{11} = -H(z-\zeta)\,\mathrm{erf}(z-\zeta)+\alpha_1\frac{\partial}{\partial r}(\phi_1^A+\phi_2^A)_{r=1}+\alpha_2\frac{\partial^2}{\partial r^2}(\phi_1^A+\phi_2^A)_{r=1}$$
$$+\alpha_3\frac{\partial^2}{\partial z^2}(\kappa_1\phi_1^A+\kappa_2\phi_2^A)_{r=1}+\alpha_4\frac{\partial}{\partial r}[(1+\kappa_1)\phi_1^A+(1+\kappa_2)\phi_2^A]_{r=1}\Big|_{z'=0}^{z'=z}, \tag{B18}$$

$$\Gamma_{12} = \alpha_1\frac{\partial}{\partial r}(\phi_1^B+\phi_2^B)_{r=1}+\alpha_2\frac{\partial^2}{\partial r^2}(\phi_1^B+\phi_2^B)_{r=1}$$
$$+\alpha_3\frac{\partial^2}{\partial z^2}(\kappa_1\phi^B+\kappa_2\phi_2^B)_{r=1}+\alpha_4\frac{\partial}{\partial r}[(1+\kappa_1)\phi_1^B+(1+\kappa_2)\phi_2^B]_{r=1}\Big|_{z'=0}^{z'=z}, \tag{B19}$$

$$\Gamma_{13} = \alpha_1 \frac{\partial}{\partial r}(\phi_1^C + \phi_2^C)_{r=1} + \alpha_2 \frac{\partial^2}{\partial r^2}(\phi_1^C + \phi_2^C)_{r=1}$$
$$+ \alpha_3 \frac{\partial^2}{\partial z^2}(\kappa_1 \phi_1^C + \kappa_2 \phi_2^C)_{r=1} + \alpha_4 \frac{\partial}{\partial r}[(1+\kappa_1)\phi_1^C + (1+\kappa_2)\phi_2^C]_{r=1}\Big|_{z'=0}^{z'=z}, \quad \text{(B20)}$$

$$\Gamma_{21} = \alpha_5 \frac{\partial}{\partial r}(\phi_1^A + \phi_2^A)_{r=1} + \alpha_6 \frac{\partial^2}{\partial r^2}(\phi_1^A + \phi_2^A)_{r=1} + \alpha_7 \frac{\partial^2}{\partial z^2}(\kappa_1 \phi_1^A + \kappa_2 \phi_2^A)_{r=1}, \quad \text{(B21)}$$

$$\Gamma_{22} = \alpha_5 \frac{\partial}{\partial r}(\phi_1^B + \phi_2^B)_{r=1} + \alpha_6 \frac{\partial^2}{\partial r^2}(\phi_1^B + \phi_2^B)_{r=1} + \alpha_7 \frac{\partial^2}{\partial z^2}(\kappa_1 \phi_1^B + \kappa_2 \phi_2^B)_{r=1}, \quad \text{(B22)}$$

$$\Gamma_{23} = \alpha_5 \frac{\partial}{\partial r}(\phi_1^C + \phi_2^C)_{r=1} + \alpha_6 \frac{\partial^2}{\partial r^2}(\phi_1^C + \phi_2^C)_{r=1} + \alpha_7 \frac{\partial^2}{\partial z^2}(\kappa_1 \phi_1^C + \kappa_2 \phi_2^C)_{r=1}, \quad \text{(B23)}$$

$$\Gamma_{31} = \frac{\partial}{\partial z}(\kappa_1 \phi_1^A + \kappa_2 \phi_2^A)_{z=0}, \quad \text{(B24)}$$

$$\Gamma_{32} = \frac{\partial}{\partial z}(\kappa_1 \phi_1^B + \kappa_2 \phi_2^B)_{z=0}, \quad \text{(B25)}$$

$$\Gamma_{33} = \frac{\partial}{\partial z}(\kappa_1 \phi_1^C + \kappa_2 \phi_2^C)_{z=0}, \quad \text{(B26)}$$

where

$$\alpha_1 = 2\nu_f \frac{C_{12}}{E_f}, \quad \text{(B27)}$$

$$\alpha_2 = 2\nu_f \frac{C_{11}}{E_f}, \quad \text{(B28)}$$

$$\alpha_3 = 1 + 2\nu_f \frac{C_{13}}{E_f}, \quad \text{(B29)}$$

$$\alpha_4 = 2\frac{C_{44}}{E_f}, \quad \text{(B30)}$$

$$\alpha_5 = (1+\nu_f)(1-2\nu_f)\frac{C_{12}}{E_f} - 1, \quad \text{(B31)}$$

$$\alpha_6 = (1+\nu_f)(1-2\nu_f)\frac{C_{11}}{E_f}, \quad \text{(B32)}$$

$$\alpha_7 = (1+\nu_f)(1-2\nu_f)\frac{C_{13}}{E_f} - \nu_f. \quad \text{(B33)}$$